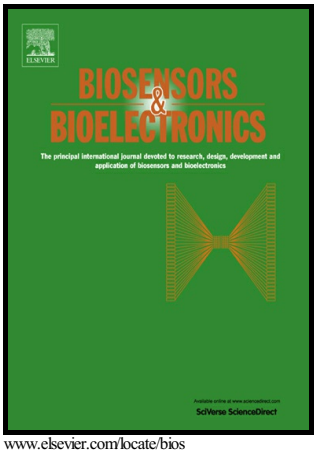

www.elsevier.com/locate/bios

Capacitive malaria aptasensor using *Plasmodium falciparum* glutamate dehydrogenase as target antigen in undiluted human serum

Naveen K. Singh, Sunil K. Arya, Pedro Estrela, Pranab Goswami

PII: S0956-5663(18)30454-8
DOI: https://doi.org/10.1016/j.bios.2018.06.022
Reference: BIOS10542

To appear in: *Biosensors and Bioelectronic*

Received date: 3 May 2018
Revised date: 2 June 2018
Accepted date: 8 June 2018

Cite this article as: Naveen K. Singh, Sunil K. Arya, Pedro Estrela and Pranab Goswami, Capacitive malaria aptasensor using *Plasmodium falciparum* glutamate dehydrogenase as target antigen in undiluted human serum, *Biosensors and Bioelectronic,* https://doi.org/10.1016/j.bios.2018.06.022

Capacitive malaria aptasensor using *Plasmodium falciparum* glutamate dehydrogenase as target antigen in undiluted human serum

Naveen K. Singh[1], Sunil K. Arya[2,1], Pedro Estrela[2*], Pranab Goswami[1*]

[1] Department of Biosciences and Bioengineering, Indian Institute of Technology Guwahati, Pin: 781039 Assam, India.

[2] Centre for Biosensors, Bioelectronics and Biodevices (C3Bio) and Department of Electronic and Electrical Engineering, University of Bath, Claverton Down, Bath BA2 7AY, United Kingdom.

pgoswami@iitg.ernet.in

p.estrela@bath.ac.uk

***Correspondence:**Tel: +91 361 2582202; Fax: +91 361 2582249.

***Correspondence:** Tel.: +44-1225-386324.

Abstract

A capacitive aptasensor for detecting the malaria biomarker, *Plasmodium falciparum* glutamate dehydrogenase (*Pf*GDH), directly in human serum samples developed. A thiolated ssDNA aptamer (NG3) that binds specifically to *Pf*GDH antigen with high affinity (K_d = 79 nM) was used to develop the aptasensor. The aptasensor produced capacitance response at an optimized frequency of 2 Hz in a non-Faradaic electrochemical impedance based signal transduction platform. The aptasensor exhibited a wide dynamic range of 100 fM - 100 nM with a limits of detection of 0.77 pM in serum samples. The interference from other predominant malarial biomarkers, namely, *Plasmodium falciparum* –lactate dehydrogenase and -histidine rich protein-II on the aptasensor was negligible. This *Pf*GDH aptasensor with highly sensitive and label free detection capability has great application potential for diagnosis of asymptotic malaria and monitoring the regression of malaria during treatment regime with antimalarial drugs.

[1] Current address: Gwent Electronic Materials Ltd, Monmouth House, Mamhilad Park, Pontypool, Torfaen NP4 0HZ. United Kingdom

Keywords- Aptamer, Biosensor, Capacitance, Surface plasmon resonance, *Pf*GDH, Malaria.

1. Introduction

Malaria is an infectious disease that occurs mostly in tropical and sub-tropical regions of the world (Margaret et al., 2017). The World Health Organization (WHO) reported that half of the total malaria related deaths occurred in the year 2015 was caused solely by the infection of the *Plasmodium falciparum* species (World Health Organization, 2016). Malaria is a curable disease provided an appropriate diagnosis and linked follow-up treatment for the suspected patients are offered on time. Till date microscopic investigation is considered as the gold standard method for malaria diagnosis. Several other methods such as ELISA, buffy coat analysis, nucleic acid amplification and rapid diagnostic test (RDT) are also utilized for diagnosis of malaria (Tangpukdee et al., 2009). However, except RDTs, all these methods are difficult to employ in point of care (POC) settings and resource limited environments as they require expensive equipment and skilled operators (Morassin et al., 2002). Most of the RDTs for malaria currently employed in POC used antibody as biorecognition molecule. These widely used antibody based RDT systems however, suffer from some limitations such as, poor stability in hot and humid climates, batch to batch variations, and are non-quantitative in nature (Jorgensen et. al., 2006, Erdman and Kain, 2008).

Over the last two decades, aptamers are evolved as potential biorecognition molecules for various analytical applications. ssDNA aptamers are short chain oligonucleotides, which can selectively bind to their target molecules with high affinity. These nucleic acid aptamers offer several advantages such as, their easy large scale production at low cost following *in vitro* chemical protocol, high thermal stability and long shelf-life, available compatible chemistry to immobilize them over sensor surfaces and scope to enhance their performance factors through chemical modifications (Kakoti and Goswami 2017; Cheung et al., 2013).

For malaria diagnosis, various marker proteins such as, lactate dehydrogenase (LDH), histidine rich protein-II (HRP-II), aldolase, and glutamate dehydrogenase (GDH) have been studied (Jain et al., 2014). Most of the RDTs available for the detection of *Plasmodium falciparum* (*Pf*) have used *Pf*HRP-II as the target antigen. However, couple of reports claimed that there are deletions of the *Pf*HRP-II gene in some of the African and Asian regions (Murillo et al., 2015; Viana et al., 2017), which prompted to explore other available biomarkers for developing reliable detection devices for the *Pf* parasite. The *Pf*GDH has been recognised as a powerful malaria biomarker due to its clear distinctions from the host GDH in terms of structure, sequence, location and enzyme kinetics (Wagner et al., 2005; Zaganas et al., 2009). Moreover, it is present in a significant quantity in soluble form in the blood serum of the patients throughout the sexual and asexual stages of the parasite development (Li et al., 2005; Dominguez and Acosta, 1996).

Electrochemical impedance spectroscopy (EIS), either in Faradaic or non-Faradaic modes, has recently received enormous interest in the field of biosensors due to its highly sensitive signal transduction feature (Wang et al., 2017; Rohrbach et al., 2012). The Faradic impedance spectroscopy however, relies on an indirect method where a redox species is used to investigate the bio interaction at the electrode interface (Liu et al., 2017). Hence, the method requires an additional design strategy or step to incorporate the redox species in the detection device, which intricate the system and thus discourage it for point of care (POC) applications. In contrast, non-Faradaic EIS measurements do not require any external redox probe, allowing direct measurement of the target molecule in the sample that makes the system suitable for POC applications (Arya et al., 2018, Luo et al., 2013). In non-Faradaic EIS measurements, variations in interfacial capacitance developed by dislocating water molecules and ions away from a bio-functionalised electrode surface after its binding to the target molecule is used for sensor application (Tkac and Davis, 2009).

Herein, a *Pf*GDH ssDNA aptamer selected through systemic evaluation of ligand exponential enrichment (SELEX) process was immobilized chemically over an electrode surface through a self-assembled technique. The developed aptasensor was then utilized for detecting *Pf*GDH directly in serum samples using non-Faradaic EIS technique. The aptasensor exhibited high sensitivity, selectivity and a wide dynamic range for the *Pf*GDH in blood serum.

2. Experimental

2.1. Materials

Potassium phosphate buffer, $MgCl_2$, NaCl, KCl, alumina powder (50 nm coarse sizes), PCR kit, streptavidin coated magnetic beads, human serum albumin (HSA) and human serum from AB positive male were procured from Sigma Aldrich. Starting blocking buffer, H_2SO_4 and Top 10 competent cells were procured from Thermo Fisher. The single stranded random N40 oligonucleotide DNA library with conserved primer binding site and primer were received from IDT technology (USA). All the proteins (*Pf*GDH, HGDH, *Pf*LDH and *Pf*HRP-II) used in the present investigation were cloned, expressed and characterised following our previous works (Chakma et al., 2016; Jain et al., 2016; Singh et al., 2018). Thiolated HPLC grade purified *Pf*GDH aptamer NG3 and NG51 (see Table 1) were get synthesised from Sigma (UK). The experiments on human blood serum samples were ethically cleared and approved by the Institute Human Ethics Committee, IIT Guwahati, India.

Table 1. Thiolated NG3 and NG51 aptamer sequences.

Aptamer	Sequences (5'→3')
NG3	SH-$(CH_2)_6$-TTT TCA CCT CAT ACG ACT CAC TAT AGC GGA TCC GAG CCG GGG TGT TCT GTT GGC GGG GGC GGT GGG CGG GCT GGC TCG AAC AAG CTT GC
NG51	SH-$(CH_2)_6$-TTT TCA CCT CAT ACG ACT CAC TAT AGC GGA CCC CAC

TCA CTG CTC GGA CTC TCC CCC TCC CCG CCT GGC TCG AAC AAG CTT GC

2.2. Aptamer selection and screening

Aptamers against the antigen *Pf*GDH were developed from a $10^{14\text{-}15}$ random ssDNA oligonucleotide library following the SELEX process as reported (Singh et al., 2018). In brief, ssDNA aptamer was selected from a random oligonucleotide library in which a random 40-nucleotide region (Fw-N40-Rev) was flanked by conserved primer binding site for amplification. A polyvinylidene difluoride (PVDF) membrane was used for *Pf*GDH immobilization. For the selection of aptamer, a total of 17 rounds of SELEX cycle were performed, out of which 3 counter SELEX cycle against PVDF membrane and 2 rounds of negative SELEX cycle with HGDH were performed to eliminate non-specific aptamers candidates. Probable aptamer candidates were cloned at the end of 17 rounds of SELEX into pGEMT easy vector and transformed into *E.coli* DH5α cells. The transform cells were selected by blue-white screening and restriction digestion. The positive clone was sequenced and the secondary structure was predicted through Mfold online software (Zuker, 2003).

2.3. Aptamer binding affinity measurement

A surface plasmon resonance (SPR) study was performed for the measurement of the dissociation constant (K_d) value of the developed aptamer against *Pf*GDH using a Reichert SPR 7000DC (USA) dual channel flow spectrophotometer at 25 °C over 50 nm gold coated chips (Reichert Technology, USA). The SPR chip was first cleaned with piranha solution (3:1 H_2SO_4: H_2O_2) for 20 s, then washed with milli-Q water (18.2 MΩ.cm, Millipore, UK) for 5 min followed by purging with N_2 gas jet for drying. The chip was then incubated overnight with thiolated aptamer (1 µM) along with 6-mercapto 1-hexanol (MCH, Sigma) in a ratio of

1:100 in binding buffer, followed by backfilling the surface with 1 mM MCH for 1 h (Aliakbarinodehi et al., 2017; Green et al., 2000). All the protein solutions and buffer were filtered through a 0.2 µm filter and degassed for 2 h. After obtaining a stable binding buffer SPR line, different concentrations of *Pf*GDH and control protein were flowed over the aptamer modified SPR chip at 25 µl/min for 10 minutes, followed by 5 min of a dissociation step with buffer to remove any unbound proteins. The buffer used for the present work is presented in the Table S1, supplementary material.

2.4. Sensor fabrication

Bare gold disc electrodes of 3 mm diameter (CHI Instruments, USA) were cleaned with piranha solution (3:1 ratio of H_2SO_4: H_2O_2) for 30 s, followed by mechanical polishing with 50 nm course size alumina slurry (Sigma) for 5 min over a polishing pad (BASi, USA). The electrodes were then sonicated in absolute ethanol and milli-Q water for 5 min each, sequentially. Thereafter, electrodes were electrochemically cleaned in 0.5 M H_2SO_4 by cycling the potential between -0.5 and +1.3 V *versus* Hg/Hg_2SO_4 till a stable characteristic reduction current peak of bare gold was observed. The electrodes were rinsed with ample amounts of milli-Q water and then dried in N_2 gas jet steam.

The aptamers were then grafted to the clean gold electrodes following a previously reported method (Jolly et al., 2017). In brief, 100 mM of MCH was first prepared in absolute ethanol as stock solution and then diluted to 1 mM in binding buffer. The aptamer was heat treated at 90 °C for 5 min, then cooled down to room temperature (RT) for 15 min before initiating the sensor fabrication. The clean electrodes were incubated in 200 µl of *Pf*GDH specific aptamer: MCH in a 1:100 ratio and left overnight in a humidity chamber. After the immobilization, electrodes were rinsed with milli-Q water to remove unbound aptamers. To ensure proper

coverage, the electrodes were further treated with 1 mM MCH for 1 h. The electrodes were again washed with milli-Q water and dried with N_2 steam and blocked with starting blocking buffer (Thermo Fisher, UK) for 30 minutes to prevent non-specific attachment of proteins over the electrodes.

2.5. EIS measurement.

Non-Faradaic EIS measurements were performed using a µAutolab III / FRA2 potentiostat (Metrohm) in a two-electrode setup consisting of aptamer functionalised gold disc as working electrode and Ag/AgCl as reference electrode. The measurements were performed in binding buffer, applying a 10 mV a.c. amplitude voltage in the frequency range of 1 MHz - 100 MHz. After obtaining a stable signal in the measurement buffer, the electrodes were incubated with varying concentrations of *Pf*GDH protein in 200 µl binding buffer for 30 min, following which the EIS spectra were recorded after washing the electrodes with buffer. Further, to examine the applicability of the sensor for real sample analysis, blocked/NG3 aptamer/gold electrodes were tested in undiluted human serum samples spiked with *Pf*GDH following the similar conditions. The specificity of the developed aptasensor was examined by challenging the aptasensor with other malaria biomarker proteins namely, *Pf*LDH, *Pf*HRP-II and analogous human GDH (HGDH) and HSA in serum sample.

3. Results and Discussion

3.1. Aptamer characterization

Two single stranded DNA aptamers NG3 and NG51 that were highly enriched when screened against the antigen *Pf*GDH in the SELEX analysis were considered in the present study. The

secondary structures of the aptamers as determined by Mfold are shown in Fig. 1 (Singh et al. 2018). The selected 5' end thiol modified aptamers were immobilized (~200 nmol) over SPR chips followed by backfilling / blocking with MCH. The prepared electrodes were then utilized for detection of different concentration of *Pf*GDH and other non-specific proteins. The binding of *Pf*GDH over the gold chip surface led to an increase in SPR angle, reaching a stabilization plateau within less than 10 mins. After binding, buffer solution was passed over the surface to remove loosely bound protein from the surface. The amount of *Pf*GDH attached to the SPR chip was calculated by recording the difference between the final and initial SPR angle (Fig. 1A, B). The specificities of the developed aptamers were analysed by testing control proteins (HGDH, *Pf*LDH, HSA), which showed negligible changes in SPR angle for both the NG3 and NG51 aptamers (Fig. S1, Supplementary material). The binding affinities of the developed aptamers were calculated using the single ligand binding site equation in 1:1 interaction mode, X+Y=XY, where X is injected target protein and Y is immobilized aptamer molecule, XY is aptamer–protein complex formed over the SPR chip. The formation of aptamer–protein complex (XY) is directly proportional to the response unit (RIU) of SPR (Scarano et al., 2010). The dissociation constant (K_d) values for the aptamers were calculated using the equation $RIU=RIU_{max}*c/(K_d+c)$, where c is the protein concentration. The K_d values were determined as 79.16 ± 1.58 nM and 370 ± 14.39 nM for NG3 and NG51, respectively. The Gibbs energy, $\delta G = - RT \ln K_a$, where R is the universal gas constant, T is temperature and $K_a = 1/K_d$, was also calculated for the NG3 and NG51 aptamers at 298 K and found to be - 56.9 kJ/mol and - 36.7 kJ/mol, respectively. The negative Gibbs energy values indicate the prompt interaction of *Pf*GDH with aptamer over the solid surface platform of the SPR chip, and found to be better for NG3 aptamer candidate. Based on the higher binding affinity against *Pf*GDH and lower Gibbs energy change, NG3 was considered for further study.

3.2. Sensor surface characterization

The sensor fabrication process over the bare gold electrodes was characterized by atomic force microscopy (AFM) and cyclic voltammetry (CV). The results of AFM characterization were done in continuous tapping mode. The topographic average roughness analysis using wsxm 5.0 software showed gradual decrease of roughness from the bare gold (1.52 nm) to aptamer modified gold electrode (1.41 nm) and blocked aptasensor electrode (1.33 nm). This was accompanied by an increase in the average height of the surface modified electrodes, indicating the binding of aptamer and blocking reagents over the electrode (Fig. 2A-C). CV was performed to investigate the layer by layer modification on the electrode surface. The results depict the quasi reversible cyclic voltammogram of $[Fe(CN)_6]^{3-/4-}$ with a decrease in oxidation and reduction currents of the modified electrodes compared to the blank gold electrode (Fig. 2D). The formation of a self-assembled monolayer of aptamer-MCH over the gold electrode led to an increase in ΔEp (difference between oxidation and reduction potentials) and lowered the redox current. This could be attributed to the charge repulsion caused by the negative phosphate backbone of the aptamer (Bang et al., 2005) as well as the passivation of the electrode hindering the electron transfer. The results suggest successful assembly of the aptamer over the electrode surface. After blocking of aptamer/MCH electrode with the starting blocking buffer, a further decrease in redox current was observed due to void spaces of gold and/or MCH being occupied by non-conducting moieties of the blocking buffer.

3.3. Detection of PfGDH

The NG3 aptamer was used for *Pf*GDH sensing following non-Faradaic impedance measurements without using any redox marker in the solution. In this mode, high values of

impedance were observed and variations in the capacitance of the system that occurred due to the binding of the aptamer with the target protein were measured. The capacitive response of the sensor was discerned by measuring $1/\omega Z''$, where ω is the angular frequency and Z'' the imaginary part of the impedance of the system. A maximum in the phase angle was observed at ~2 Hz, indicating maximum capacitive response at this frequency (Fig. 3A). This frequency was thus used for plotting the dose dependent response of the capacitive signal change. The reduction in capacitance with increasing concentrations of *Pf*GDH indicates successful binding of the target molecule with the NG3 aptamer (Fig. 3B, C). The change in capacitance is attributed to the alteration in dielectric properties of the biolayer through the replacement of solvated ions and water molecules by the protein, as well as due to the increase in thickness of the biolayer upon protein binding (Arya et al., 2018; Liu et al., 2017). The limit of detection (LOD) (3x standard deviation of blank/slope of calibration curve) of *Pf*GDH was found to be 0.43 pM in the buffer, with a linear (in log scale) detection range of 100 fM - 100 nM (Fig. 3D.). The sensitivity of the developed capacitive aptasensor was compared with NG3 immobilized SPR sensor by analysing *Pf*GDH at concentrations of 1nM and 100 nM in buffer medium (Fig. S2, supplementary material). The sensitivity of both the aptasensor was comparable at higher concentration (100 nM) of the antigen. However, at lower concentration (1 nM) of PfGDH, the sensitivity of the SPR sensor was negligible, while at this concentration the capacitive aptasensor exhibited ~62 % of the sensitivity at 100 nM of *Pf*GDH. The results confirmed the higher sensitivity of the capacitive aptasensor than the SPR aptasensor at lower concentration range of the antigen.

The capacitive aptasensor was then tested directly in undiluted blood serum with spiked *Pf*GDH. The *Pf*GDH protein with different concentrations that fall within the dynamic range obtained in the buffer medium (100 fM - 100 nM) was used in the undiluted serum (Fig. 4). This range covers the previously reported *Pf*GDH concentrations used (2 to 16 nM) for

malaria diagnosis through an immuno-chromatographic dipstick based method (Djadiad et al., 2014; Li et al., 2005). Like in buffer, a maximum phase angle was observed at ~2 Hz during the measurement of *Pf*GDH protein in serum samples (Fig. 4A). The capacitance at 2 Hz was therefore considered further for generating the calibration curve (Fig. 4B). The detection of *Pf*GDH in serum also followed a linear dependency of its concentration in the range with the capacitance signal and an LOD of 0.77 pM for *Pf*GDH was discerned (Fig. 4C). Moreover, the sensitivity of the aptasensor as derived from the slopes of the calibration curves in serum and buffer samples were 0.12 (10^{-7}F)/ log ([*Pf*GDH] pM) and 0.09 (10^{-7}F)/ log([*Pf*GDH] pM), respectively. The results indicate a comparable signal sensitivity of the aptasensor between samples in buffer and serum media, which validate a conducive microenvironment for the interaction of the aptamer with the target antigen protein in the serum medium (Park et al., 2012). The binding between *Pf*GDH and NG3 aptamer over the electrode surface is likely to be facilitated by the interaction between some positively charged *Pf*GDH amino acid residues and the negatively charged ssDNA aptamer. The net surface charge of aptamer-protein complex governed the dielectric property over the sensing surface of electrode which was not affected by the ionic microenvironment in serum in the present case (Cole and Cole, 1941; Pethig and Kell, 1987). The interferences from the other prominent malaria biomarker proteins (*Pf*LDH and HRP-II) that are likely to be secreted during the diseased condition were examined by spiking these proteins in undiluted serum (Fig. 4D). The responses were 6.5% (*Pf*LDH) and 0.5% (*Pf*HRP-II) of the control protein (*Pf*GDH) for the corresponding proteins shown in the parentheses. The result indicates only a minor non-specific interaction of the sensor with the *Pf*LDH protein. The sensitive response profile obtained directly on the serum sample indicates that the serum components including HGDH and the predominant serum protein, HSA do not significantly interfered the aptasensor function. There are limited reports on the malaria diagnostic device targeting the

*Pf*GDH antigen (Seol et al., 2017). An antibody based immuno chromatographic technique exploiting gold nanoparticles as optical probe could offer a detection range of 0.62-5µg/ml for *Pf*GDH (Li et al., 2005). Recently, a protein induced fluorescence enhancement based detection of *Pf*GDH using carbon dot coupled specific aptamer has been reported (Singh et al, 2018). The technique could offer a dynamic range of 1-25nM with an LOD of 2.85 nM. Hence, the present aptasensor exhibited superior performance both in terms of LOD and dynamic range than the previous reports.

4. Conclusion

A capacitive aptasensor for selective detection of the malaria biomarker, *Pf*GDH in undiluted human serum samples was developed following the scheme shown in the figure 5. The aptasensor generated a non-Faradaic EIS signal following its binding with the target antigen (*Pf*GDH). The capacitive signal change was linearly correlated with a wide concentration range of the antigen (100 fM - 100 nM). The aptasensor offered an LOD for the antigen in picomolar level. This is the first report on *Pf*GDH aptasensor exploiting non-Faradaic impedance as sensing signal. The chemical technique adapted here for the immobilization of the aptamer over the electrode surface facilitated easy and reproducible fabrication of the aptasensor. This label-free aptasensor with ultra-low LOD has great application potential for diagnosis of asymptomatic malaria and for monitoring the regression of malaria during treatment regime with antimalarial drugs. We envisioned that with the advent of advance state-of-art electrochemical technology, the instrument for measuring the capacitance could be scaling down to an appropriate size for converting the developed aptasensor to a hand-held device suitable for application in POC settings and resource limited environments.

Acknowledgements

N.K.S. acknowledges support from the DBT, India and the British Council in the form of a Newton-Bhabha PhD Placement Grant (2016-17). S.K.A. was funded by a Marie Skłodowska-Curie Individual Fellowship through the European Commission's Horizon 2020 Programme (grant no. 655176).

Appendix A. Supplementary material:

Supplementary data associated with this article.

References

Aliakbarinodehi, N., Jolly, P., Bhalla, N., Miodek, A., De Micheli, G., Estrela, P., Carrara, S., 2017. Sci. Rep. 7, 44409.

Arya, S. K., Zhurauski, P., Jolly, P., Batistuti, M. R., Mulato, M., Estrela, P., 2018. Biosens. Bioelectron. 102, 106–112.

Bang, G. S., Cho, S., Kim, B., 2005. Biosens. Bioelectron. 21, 863–870.

Chakma, B., Jain, P., Singh, N.K., Goswami, P., 2016. Anal. Chem. 88 (20), pp 10316–10321.

Cheung, Y. W., Kwok, J., Law, A. W. L., Watt, R. M., Kotaka, M., Tanner, J. A., 2013. Proc. Natl. Acad. Sci. USA 110, 15967–72.

Cole, K. S., Cole, R. H., 1941 J. Chem. Phys. 9 (4), 341-351.

Djadiad, N. D., Sedighion, F., Raj, A., Zakeri, S., 2014. US patent. US 2014/0248629 A1.

Dominguez, N. D., Acosta, A. R.,1996. Kor. J. Parasitology, 34 (4), 239-246.

Erdman, L. K., Kain, K. C., 2008. Travel Med. Infect. Dis. 6, 82–99.

Green, R. J., Frazier, R. A., Shakesheff, K. M., Davies, M. C., Roberts, C. J., Tendler, S. J.

B., 2000. Biomaterials 21, 1823–1835.

Jain, P., Chakma, B., Patra, S., Goswami, P., 2014. Biomed Res. Int. 2014, 852645.

Jain, P., Chakma, B., Singh, N.K., Patra, S., Goswami, P., 2016. Mol. Biotechnol. 58 (7), 497-508.

Jorgensen, P., Chanthap, L., Rebueno, A., Tsuyuoka, R., Bell, D., 2006. Am. J. Trop. Med. Hyg. 74, 750–754.

Kakoti, A., Goswami, P., 2017. Biochimica et Biophysica Acta - General Subjects, 1861(1), 3289–3299.

Li, Y., Ning, Y. S., Li, L., Peng, D. O., Dong, W. Q., Li, M., 2005. Di Yi Jun Yi Da Xue Xue Bao 25 (4), 435-438.

Liu, B., Lu, L., Hua, E., Jiang, S., Xie, G., 2012. Microchim. Acta 178, 163–170.

Liu, J., Chisti, M.M., Zeng, X., 2017. Anal. Chem. 89, 4013–4020.

Margaret, A. P, Jeremy, N. B., Manyando, C., van Huijsduijnen, R. H., Van Voohis, W. C., Wells, T. N. C., 2017. Nat. Rev. Dis. Primers 3, 17050.

Morassin, B., Fabre, R., Berry, A., Magnaval, J. F., 2002. Am. J. Trop. Med. Hyg. 66, 503–508.

Murillo, S. C., Sheila, A. O., Joseph, F. A., Zuleima, P., Erika, D., Sandra. I., Curtis, S. H., Alexandre, M. O., David, B., Venkatachalam, U. K., Barnwell, J. W., 2015. PLoS One 10 (7), e0131576.

Park, J.W., Saravan K. S., Niazi, J. H., Gurbuz, Y., Youn, B. S., Gu, M. B., 2012. Biosens. Bioelectron. 38, 233–238.

Jolly, P., Formisano, N., Tkac, J., Kasák, P., Frost, C. G., Estrela, P., 2015. Sens. Actuators B 209, 306-312.

Pethig, R., Kell, D., 1987. Phys. Med. Biol. 32, 933-970.

Rohrbach, F., Karadeniz, H., Erdem, A., Famulok, M., Mayer, G., 2012. Anal. Biochem. 421, 454–459.

Scarano, S., Mascinia, M., Turner, A. P. F., Minunnia, M., 2010. Biosens. Bioelectron. 25 (5), 957-966.

Seol, B., Shin, H. I., Kim, J. Y., Jeon, B. Y., Kang, Y. J., Pak, J. H., Kim, T. S., Lee, H. W., 2017. Malar. J. 16, 3.

Singh, N. K., Chakma, B., Jain, P., Goswami, P., 2018. ACS Comb Sci. DOI: 10.1021/acscombsci.8b00021.

Tangpukdee, N., Duangdee, C., Wilairatana. P., Krudsood, S., 2009. Korean J Parasitol. 47 (2), 93-102.

Tkac, J., Davis, J. J., Davis, J. J., 2009. The Royal Society of Chemistry, pp. 193–224.

Viana, G. R., Akinyi, O. S, Silva, F. L, Lima, B. D, Macedo, O. A, Goldman, I. F., 2017. PLoS ONE 12 (3), e0171150.

Wagner, J. T., Lüdemann, H., Färber, P. M., Lottspeich, F., Krauth, S. R., 1998. Eur. J. Biochem, 258, 813-819.

Wang, L., Veselinovic, M., Yang, L., Geiss, B. J., Dandy, D. S., Chen, T., 2017. Biosens. and Bioel, 87, 646-653.

World Health Organization, 2016. World Malaria Report 2016. World Health Organization: Geneva. Available from http://www.who.int/malaria/publications/world-malaria-report-2016/report/en/; assessed April 2018.

Zaganas, I., Spanaki, C., Plaitakis, A., 2012. Neurochem. Int. 61, 455–462.

Zuker, M., 2003. Nucleic Acids Res. 31, 3406–3415.

Figures

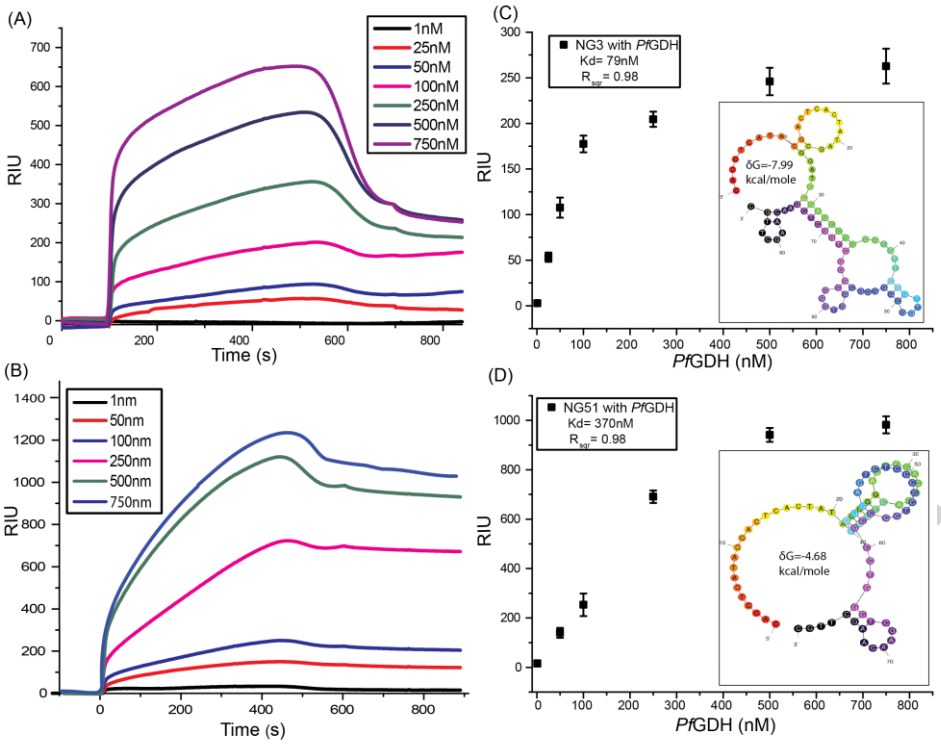

Fig. 1. SPR sensogram for NG3 (A) and NG51 (B) with different concentration of *Pf*GDH. Plotting of sensogram data for determination of dissociation constant (K_d) for (C) NG3 and (D) NG51. Inset secondary structure of NG3, NG51 aptamer along with δG values.

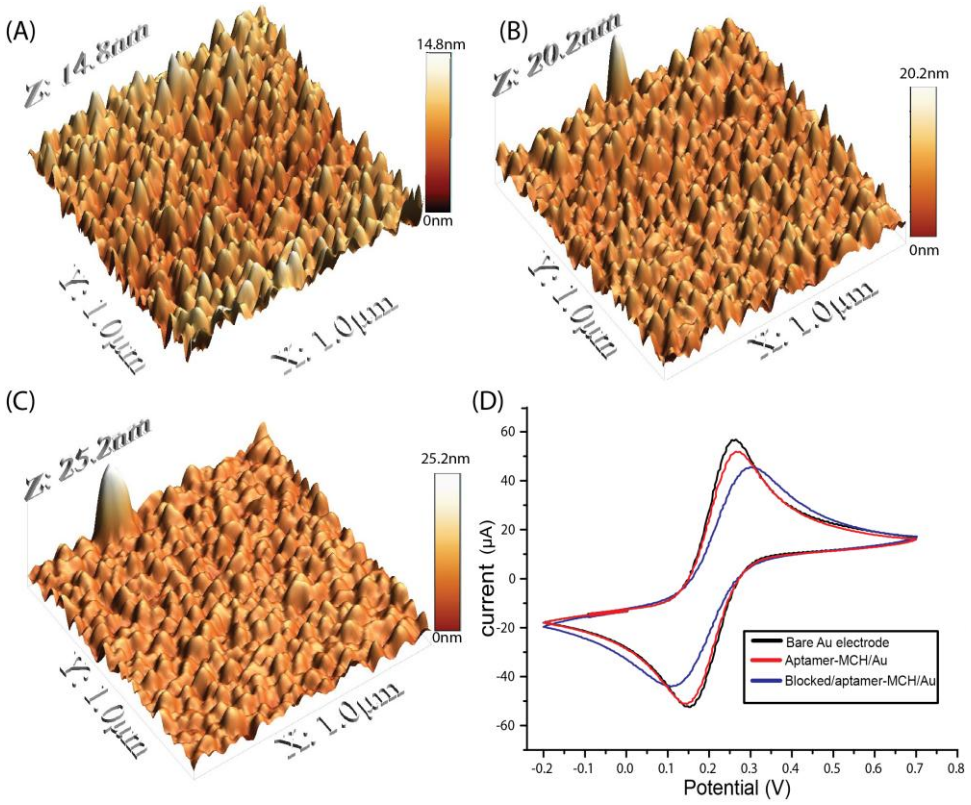

Fig. 2. AFM images of (A) bare gold electrode (B) surface assembled monolayer with aptamer-MCH over gold electrode (C) surface blocking with MCH and blocking buffer over aptamer modified electrode. (D) CV of the electrodes recorded by using Ag/AgCl as reference electrode. Scan rate of 50 mV/s in 10 mM potassium hexacyanoferrate solution prepared in PBS.

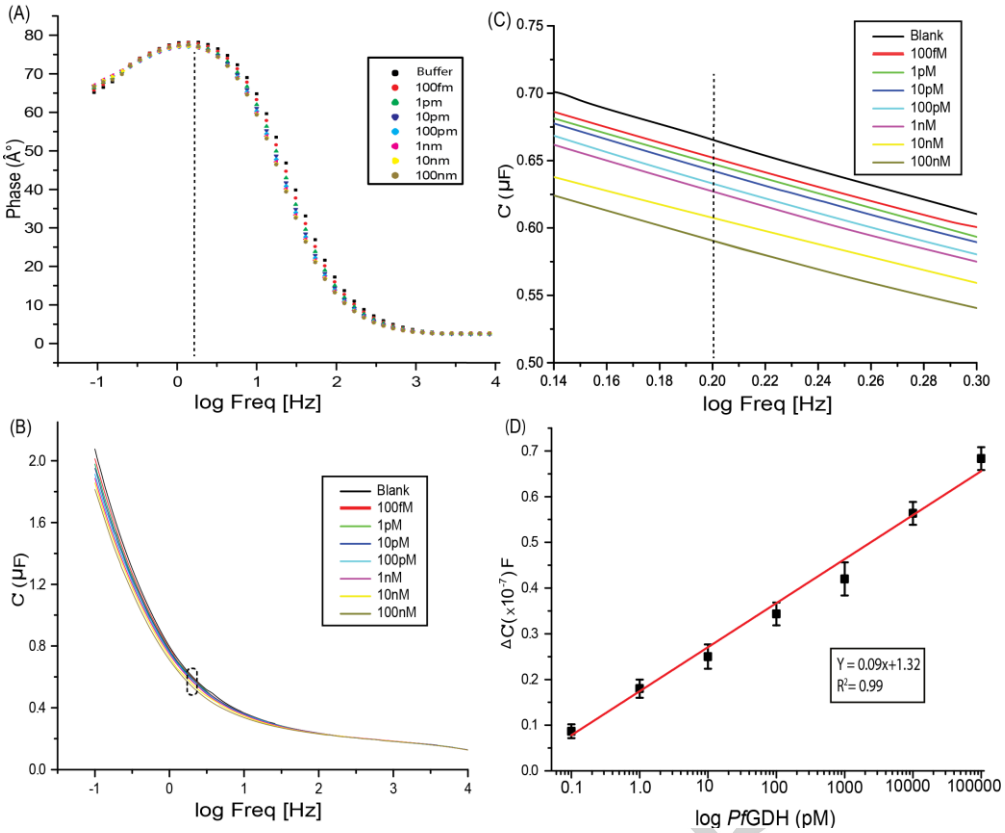

Fig. 3. Non-Faradaic measurement in buffer (A) Phase response vs frequency, (B) Capacitance response of NG3 aptamer-*Pf*GDH with circled enlarged image in inset. (C) Enlarged image of circled region of capacitance responses. (D) Calibration curve of capacitance response at 2 Hz versus log *Pf*GDH concentrations spiked in buffer.

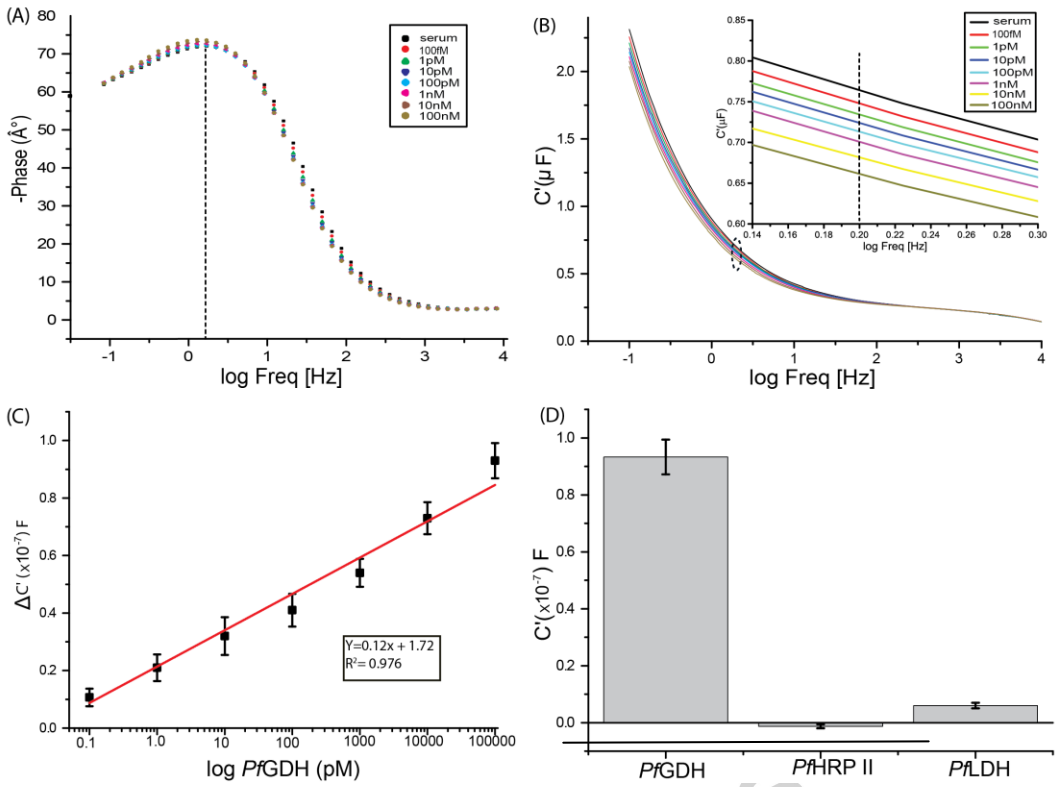

Fig. 4. (A) Non-Faradaic measurement in undiluted serum Phase response vs frequency. (B) Capacitance response of NG3 aptamer-*Pf*GDH with circled enlarged image in inset. (C) Calibration curve of capacitance response at 2 Hz verses log *Pf*GDH concentrations spiked in undiluted serum. (D) Response of NG3 aptamer with analogue proteins each with 100 nM spiked in serum.

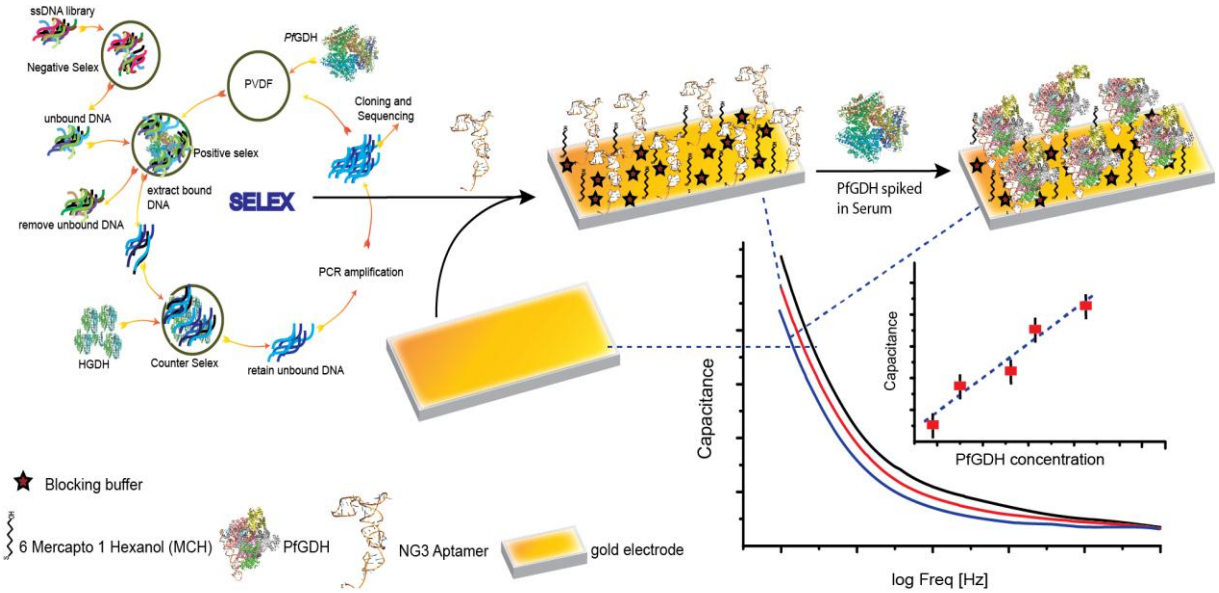

Fig. 5. Fabrication of electrode with aptamer and detection of *Pf*GDH, development of aptamer through SELEX.

HIGHLIGHTS

1. A capacitive aptasensor for detecting malaria in undiluted serum sample was developed.
2. The aptasensor was fabricated by immobilizing ssDNA aptamer over electrode through SAM technique.
3. A non-Faradaic electrochemical impedance based technique was exploited to generate the response.
4. The aptasensor exhibited limit of detection for serum *Pf*GDH in pico-molar level.
5. This *Pf*GDH aptasensor has great application potential for diagnosis of asymptotic malaria.